

Article

Rate Constants for the Reaction of OH Radicals with Hydrocarbons in a Smog Chamber at Low Atmospheric Temperatures

Lei Han ^{*,†} , Frank Siekmann and Cornelius Zetzsch ^{*,†}

Atmospheric Chemistry Research Laboratory, University of Bayreuth, 95447 Bayreuth, Germany; franck.siekmann@gmail.com

* Correspondence: leihan.net@gmail.com (L.H.); cornelius.zetzsch@mpic.de (C.Z.)

† Current address: Department of Multiphase Chemistry, Max Planck Institute for Chemistry, 55128 Mainz, Germany.

Received: 18 July 2018; Accepted: 14 August 2018; Published: 18 August 2018



Abstract: The photochemical reaction of OH radicals with the 17 hydrocarbons *n*-butane, *n*-pentane, *n*-hexane, *n*-heptane, *n*-octane, *n*-nonane, cyclooctane, 2,2-dimethylbutane, 2,2-dimethylpentane, 2,2-dimethylhexane, 2,2,4-trimethylpentane, 2,2,3,3-tetramethylbutane, benzene, toluene, ethylbenzene, *p*-xylene, and *o*-xylene was investigated at 288 and 248 K in a temperature controlled smog chamber. The rate constants were determined from relative rate calculations with toluene and *n*-pentane as reference compounds, respectively. The results from this work at 288 K show good agreement with previous literature data for the straight-chain hydrocarbons, as well as for cyclooctane, 2,2-dimethylbutane, 2,2,4-trimethylpentane, 2,2,3,3-tetramethylbutane, benzene, and toluene, indicating a convenient method to study the reaction of OH radicals with many hydrocarbons simultaneously. The data at 248 K (*k* in units of $10^{-12} \text{ cm}^3 \text{ s}^{-1}$) for 2,2-dimethylpentane (2.97 ± 0.08), 2,2-dimethylhexane (4.30 ± 0.12), 2,2,4-trimethylpentane (3.20 ± 0.11), and ethylbenzene (7.51 ± 0.53) extend the available data range of experiments. Results from this work are useful to evaluate the atmospheric lifetime of the hydrocarbons and are essential for modeling the photochemical reactions of hydrocarbons in the real troposphere.

Keywords: OH radicals; smog chamber; rate constant; hydrocarbons; low temperatures

1. Introduction

Great quantities of volatile organic compounds (VOCs) are emitted into the atmosphere from both anthropogenic and natural sources. Their atmospheric concentrations are influenced by chemical reactions in the atmosphere, where the main removal pathway for alkanes and alkylated aromatics occurs through chemical oxidation by OH radicals [1,2]. In the past few decades, many studies have been focused on the atmospheric reaction of OH radicals with alkanes and aromatics [3–13] since these kinetic data are important to estimate the lifetime of the VOCs in the atmosphere.

Smog chamber studies have started in the 1950s after the London smog episode [14]. At the beginning, they were designed mainly to study the gas-phase reactions with ozone and the chemistry of NO_x in the troposphere and the formation of aerosol from the gaseous pollutants [15–17]. Later research concentrated on the reactions of VOCs with OH radicals and their role in ozone formation and photochemical smog [18–20]. Despite intensive research on gas-phase kinetics during the last decades, comparatively little is known about the reactivity of OH radicals with VOCs below room temperature, especially for larger molecules [4,21–23]. Based on the standard atmospheric values specified by the International Civil Aviation Organization (ICAO), the sea level temperature is 288 K [24] and

drops by approximately 6.5 K per kilometer of altitude up to the tropopause [14]. However, very few hydrocarbons have been investigated at temperatures below 290 K, which are representative of the troposphere. The understanding of kinetics at low temperature is of great importance to understand the real atmospheric degradation of organic compounds.

There has been theoretical research about the reaction of OH with hydrocarbons [6,25,26], giving guidance to understand the kinetics at low temperatures. Subsequent to an extensive review on the reactions of alkanes and cycloalkanes with OH by Atkinson [27], there are only a few studies below room temperature. DeMore and Bayes [4] measured the relative rate constant of *n*-butane, *n*-pentane, and other cyclic hydrocarbon at temperatures down to 233 K. Harris and Kerr [21] developed a flow reactor system to study the relative rate constant of OH radicals with *n*-pentane, 2,2-dimethylbutane, and several other hydrocarbons, over a temperature range of 243–328 K. Talukdar et al. [22] measured the rate constant of *n*-butane and *n*-pentane over the temperature range of 212–380 K by using the pulsed photolysis laser induced fluorescence (PP-LIF) technique. Li et al. [28] studied *n*-octane, *n*-nonane, and *n*-decane relative to 1,4-dioxane at temperatures down to 240 K and Crawford et al. [29] studied the reactions of OH radicals with *n*-hexane and *n*-heptane at 240–340 K. Wilson et al. [30] studied the reactions of several alkanes and cycloalkanes with hydroxyl radicals in a photochemical glass reactor with GC/MS detection at temperatures down to 241 K. Cyclooctane and other alkanes were studied by Sprengnether et al. [31] at temperatures down to 237 K in a high-pressure flow reactor with LIF detection, and by Singh et al. [32] in a discharge flow reactor at temperatures down to 240 K. Tully et al. [23] studied the absolute rate constant of OH radicals with benzene and toluene at temperature down to 213 K, and Witte et al. [33] obtained similar results for benzene at 239–352 K. Semadeni et al. also studied the OH reactivity of benzene by using toluene as a reference compound at 274–363 K. Mehta et al. [34] measured the rate constant of OH with *o*- and *p*-xylene at 240–340 K, by using the relative rate/discharge flow/mass spectrometry (RR/DF/MS) technique. Alarcón et al. [35] used the flash photolysis resonance fluorescence technique (FPRF) to study the reaction of OH radicals with methylated benzenes including *p*-xylene, delivering an Arrhenius expression of the absolute rate constants between 300 and 350 K. A table with information on the various research conducted at low temperatures is available in Supporting Information (SI, Table S1).

In this work, we have investigated the gas phase reaction of OH with several alkanes and aromatic compounds at 288 K (sea level temperature) and 248 K (in the free troposphere this temperature corresponds to a height of approximately 5–8 km, depending on latitude and season [36]). Using *n*-pentane [27] and toluene [37] as reference compounds, the rate constants for the reactions of OH radicals with the 17 compounds have been obtained at 248 and 288 K. These two compounds are chosen as reference compounds, because their temperature-dependent parameters are well investigated between 220 to 350 K. Those data deliver chemical kinetic information about the temperature range below room temperature, and therefore are supplementary to the existing Arrhenius expression.

2. Experiments

2.1. Description of the Simulation Chamber

The simulation chamber is located at the Atmospheric Chemistry Research Laboratory of the University of Bayreuth in a temperature controllable room, where the temperature could be set from 298 K to 248 K with the aid of an inside cooling system in the room and monitored by a thermistor Epcos NTC 50 K, calibrated against a platinum resistance thermometer (Keithley 195A with probe 8693) from -40 °C to $+30$ °C. The chamber consists of four cylinder sections made of glass (Duran, Schott, inner diameter 1 m, total height 4 m), yielding a volume of 3.2 m³. Sixteen fluorescent lamps (Osram Eversun, 80 W each, kept at 300 K by an air thermostat) were employed as light sources, irradiating the chamber from the bottom through Teflon film (FEP 200A). The emission spectrum of the lamps has a Gaussian shape with a maximum at 350 nm, it starts at 300 nm and extends beyond 450 nm, containing the emission lines of mercury. The inherent heating effects on the bottom caused by the lamps led to a

vertical temperature gradient, enhancing the mixing efficiency. Sensors in the middle and upper part of the chamber measured the temperature and a ventilator was installed in the middle of the chamber to accelerate further mixing. The temperature regulation leads to variations of ± 1 K in the refrigerated laboratory. A schematic diagram of the simulation chamber is shown below (Figure 1).

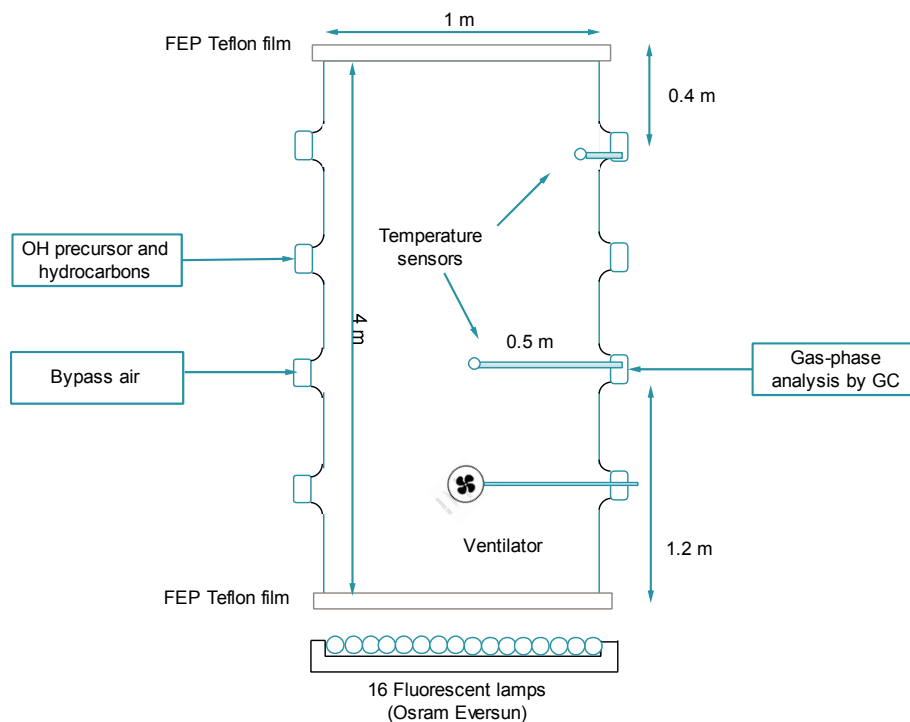


Figure 1. Schematic of the low temperature smog chamber facility. The hydrocarbons were injected into the smog chamber via syringes from two stock mixtures (see text), the gas-phase compounds were sampled through a stainless steel capillary and analyzed by GC-FID with sample enrichment (see below). Purified air was supplied via the aid of a bypass.

2.2. Instrumentation and Chemical Materials

The concentration of the hydrocarbons (starting with approx. 20 ppb each) was monitored by a gas chromatograph (GC) with a flame ionization detector (FID). It uses an automated cryogenic sample enrichment system with liquid nitrogen [10], that has been modified by substituting the 6-port valve by two magnetic valves (for detailed information see Figure S1 in Supporting Information, SI). A gas sample of 30 mL was taken every 30 min. The GC (Sichromat II, Siemens, Munich, Germany) is equipped with a capillary column (Al₂O₃-PLOT, Chrompack/Agilent) with 50 m length and an inner diameter of 0.32 mm, using N₂ as carrier gas at a column temperature of 190 °C and a FID temperature of 270 °C. In order to inject the 17 hydrocarbons *n*-butane, *n*-pentane, *n*-hexane, *n*-heptane, *n*-octane, *n*-nonane, cyclooctane, 2,2-dimethylbutane, 2,2-dimethylpentane, 2,2-dimethylhexane, 2,2,4-trimethylpentane, 2,2,3,3-tetramethylbutane, benzene, toluene, ethylbenzene, *p*-xylene, *o*-xylene, and *n*-perfluorohexane (inert standard) simultaneously into the chamber, two glass containers were employed as a storage device for preparing stock mixtures, which minimized the operating deviation during the injection process (see SI Section S1). Methyl nitrite was self-synthesized [38] and used as a photochemical precursor of the OH radicals. Two gas containers (1.3 L of each) were connected in series to approximate a constant concentration of OH (see Figure S2 in SI).

2.3. Calculation of the Reaction Rate Constant of OH with Hydrocarbons

In this study, the relative rate method was used to calculate the rate constant of the OH radical with the hydrocarbons. Assuming that the decrease of hydrocarbons in the chamber is caused by the reaction with OH radicals and by the dilution from the gas sampling process, one gets the following simple reaction scheme:



to be described by the differential equation

$$\frac{d[\text{HC}]}{[\text{HC}]} = -k_{\text{OH}}^{\text{HC}}[\text{OH}] \cdot dt - k_{\text{dil}} \cdot dt \quad (3)$$

where [HC] and [OH] represent the concentration of hydrocarbon and OH radicals at time t , respectively, $k_{\text{OH}}^{\text{HC}}$ is reaction rate constant of target hydrocarbon with OH and k_{dil} includes other changes that cause the decrease of the hydrocarbons (e.g., dilution, wall adsorption). By using n -perfluorohexane (PFH) as an internal standard, we corrected the hydrocarbon data for the dilution of the chamber contents by the gas consumption of the gas analyzers for ozone and NO_x , eliminating the second term from Equation (3). Integration then leads to the simple equation

$$\ln \frac{[\text{HC}']_0}{[\text{HC}']_t} = k_{\text{OH}}^{\text{HC}} \int [\text{OH}] dt \quad (4)$$

where $[\text{HC}']_t$ and $[\text{HC}']_0$ are the dilution-corrected concentrations of the target hydrocarbon at time t and time zero, respectively, according to $[\text{HC}'] = [\text{HC}] [\text{PFH}]_0 / [\text{PFH}]$.

The presence of several hydrocarbons in the same experiment opens the opportunity to select one of those as a reference compound (REF), in order to eliminate the time integral of OH and to obtain relative rate constants, $k_{\text{OH}}^{\text{HC}} / k_{\text{OH}}^{\text{REF}}$, from the equation:

$$\ln \frac{[\text{HC}']_t}{[\text{HC}']_0} = \frac{k_{\text{OH}}^{\text{HC}}}{k_{\text{OH}}^{\text{REF}}} \ln \frac{[\text{REF}']_t}{[\text{REF}']_0} \quad (5)$$

where $[\text{REF}']_t$ and $[\text{REF}']_0$ are the (by PFH, see above) dilution-corrected concentrations of the reference compound (n -pentane and toluene in this study) at time t and time zero, respectively. From the plots of $\ln([\text{HC}']_t / [\text{HC}']_0)$ versus $\ln([\text{REF}']_t / [\text{REF}']_0)$, straight lines are expected with zero intercept, and the slopes represent the relative rate constants. Based on the known reaction rate constant of the reference compound, $k_{\text{OH}}^{\text{REF}}$, the OH reaction rate constant of the target hydrocarbon $k_{\text{OH}}^{\text{HC}}$ can be calculated.

3. Results

In relative rate constant measurements, the FID peak area represents the concentration of each sampling point. Figure 2 shows the hydrocarbon concentrations (corrected for dilution) from one single experiment at 288 K. Following Equation (5), one can get a straight line from a plot of $\ln([\text{HC}']_0 / [\text{HC}']_t)$ of the hydrocarbons versus $\ln([\text{REF}']_0 / [\text{REF}']_t)$ for the reference compound in most cases. Three experiments were carried out at 288 K, and two experiments were performed at 248 K. The rate constants were calculated from the experimental data from all runs at each temperature (Figure 3 for straight-chain hydrocarbons, with toluene as reference compound). Table 1 summarizes results obtained for the reaction from OH with the hydrocarbons at 288 K and the results at 248 K are summarized in the supporting material (Table S2), using n -pentane and toluene as reference compounds, respectively.

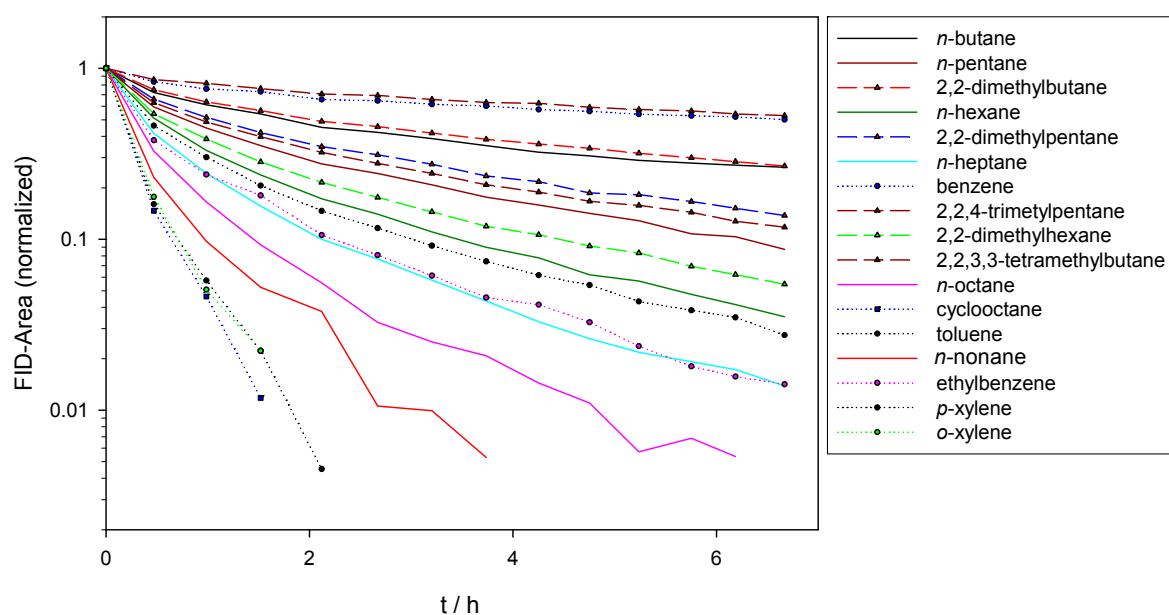


Figure 2. Decrease of hydrocarbon concentrations (normalized by *n*-perfluorohexane) during a smog chamber run by reaction with OH at 288 K (corresponding information at 248 K is displayed in the SI).

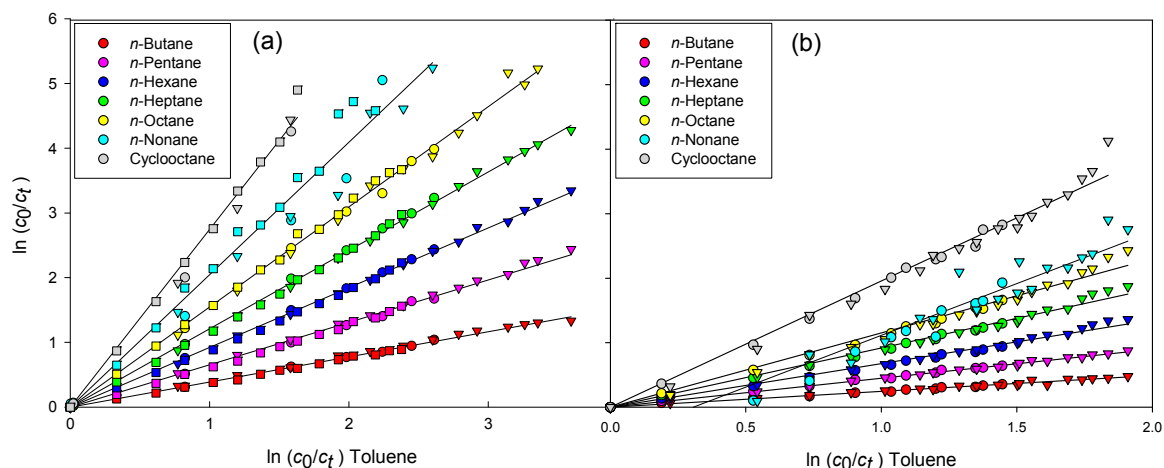


Figure 3. Plot of $\ln(c_0/c_i)$ of straight-chain alkanes and cyclooctane versus toluene (reference substance). (a) Data points of three experimental runs at 288 K; (b) Data points of two experimental runs at 248 K. The curvature of the data and the non-zero intercept for *n*-nonane at 248 K indicate experimental limitations of adsorption in the sampling capillary of the gas chromatograph. The symbols ∇ , \circ and \square distinguish data points from different experimental runs, plots of branched-chain alkanes and aromatic hydrocarbons are displayed in the SI.

At a temperature of 248 K, the initial decrease by exposure to OH appeared to be delayed for compounds with lower vapor pressures, such as *n*-nonane (Figure 3b) and *p*-xylene and *o*-xylene (SI, Figure S5b). This is possibly due to adsorption in the sampling capillary of the gas chromatograph (stainless steel, 1/16 inch, 5 m long) that was not heated during the experiments.

Table 1. Rate constants for the reaction of OH radicals with hydrocarbons at 288 K.

Compound	Rate Constant, ($k_{\text{OH}} \pm 2\sigma$)/ $10^{-12} \text{ cm}^3 \text{ s}^{-1}$		
	Toluene as Reference ^a	Pentane as Reference ^b	Average
<i>n</i> -Butane	2.28 ± 0.02	2.05 ± 0.03	2.16 ± 0.04
<i>n</i> -Pentane	3.84 ± 0.04	3.62 ^b	3.73 ± 0.04
<i>n</i> -Hexane	5.41 ± 0.03	5.25 ± 0.05	5.33 ± 0.06
<i>n</i> -Heptane	7.10 ± 0.04	6.79 ± 0.06	6.94 ± 0.07
<i>n</i> -Octane	9.07 ± 0.08	8.62 ± 0.13	8.84 ± 0.15
<i>n</i> -Nonane	12.0 ± 0.4	11.5 ± 0.5	11.8 ± 0.6
Cyclooctane	16.1 ± 0.4	15.8 ± 0.5	15.9 ± 0.6
2,2-Dimethylbutane	2.11 ± 0.02	2.04 ± 0.02	2.07 ± 0.03
2,2-Dimethylpentane	3.21 ± 0.03	3.14 ± 0.04	3.18 ± 0.05
2,2-Dimethylhexane	4.74 ± 0.03	4.57 ± 0.04	4.66 ± 0.05
2,2,4-Trimethylpentane	3.48 ± 0.03	3.35 ± 0.03	3.41 ± 0.04
2,2,3,3-Tetramethylbutane	1.01 ± 0.02	0.98 ± 0.01	1.00 ± 0.02
Benzene	1.11 ± 0.02	1.04 ± 0.01	1.08 ± 0.02
Toluene	5.86 ^a	5.52 ± 0.06	5.69 ± 0.06
Ethylbenzene	6.95 ± 0.08	6.72 ± 0.15	6.83 ± 0.17
<i>p</i> -Xylene	16.0 ± 0.9	15.4 ± 1.1	15.7 ± 1.4
<i>o</i> -Xylene	15.6 ± 0.7	15.2 ± 0.9	15.4 ± 1.1

^a k (toluene) = $1.8 \times 10^{-12} e^{340/T} \text{ cm}^3 \text{ molecule}^{-1} \text{ s}^{-1}$ (210–350 K) and $5.86 \times 10^{-12} \text{ cm}^3 \text{ molecule}^{-1} \text{ s}^{-1}$ at 288 K [37]; ^b k (*n*-pentane) = $2.52 \times 10^{-17} T^2 e^{158/T} \text{ cm}^3 \text{ molecule}^{-1} \text{ s}^{-1}$ (220–760 K) and $3.62 \times 10^{-12} T^2 e^{361/T}$ at 288 K [27].

4. Discussion

The rate constants for the reactions of the hydrocarbons with OH radicals derived from this study are plotted together with literature data in Arrhenius diagrams for the *n*-alkanes and cyclooctane (Figure 4), branched-chain alkanes (Figure 5), and aromatic hydrocarbons (Figure 6).

In order to compare to previous evaluations, the regression lines from the Arrhenius expressions for each hydrocarbon are displayed in the figures. Detailed explanations and illustrations for the alkanes and cycloalkanes can be found in the review article by Atkinson [27]. Our results demonstrate that the rate constants obtained in the present study generally agree well with the literature data, which prove that the experimental method is reliable. Moreover, the experimental results complement existing gas-phase kinetic data for hydrocarbons in the following points:

(1) For *n*-alkanes, results from this work follow the existing Arrhenius expressions quite well (Figure 4). The rate constants decrease as the temperature decreases, showing a positive correlation of temperature with the reactivity. For *n*-hexane, Atkinson [27] has recommended two Arrhenius expressions: ① k (*n*-hexane) = $2.29 \times 10^{-11} e^{-(442 \pm 52)/T} \text{ cm}^3 \text{ molecule}^{-1} \text{ s}^{-1}$, ② k (*n*-hexane) = $2.54 \times 10^{-14} T e^{-(112 \pm 28)/T} \text{ cm}^3 \text{ molecule}^{-1} \text{ s}^{-1}$. The rate constants obtained from this work at 288 K and 248 K confirm that a third type of Arrhenius expression ($k = AT^2 e^{-B/T}$) does also fit to the existing data (③ $k = 1.82 \times 10^{-17} T^2 e^{361/T} \text{ cm}^3 \text{ molecule}^{-1} \text{ s}^{-1}$ [27]). More experimental data are needed (especially at high temperatures) to determine a more appropriate temperature dependence relationship from the existing Arrhenius expressions. Data reported by Crawford et al. [29] for *n*-hexane are away from expression ③ and in case of *n*-heptane, their data are also lower than the recommended Arrhenius expression, indicating a systematic deviation. When using only *n*-hexane as reference compound, our result at 248K for *n*-heptane agrees to the results of Crawford et al. and Wilson et al. (see SI, Figure S6). In addition, we compared the different results when using *n*-butane, *n*-pentane, and *n*-hexane as reference compounds respectively. The calculated rate constant decrease with increasing CH₂ chains: 7.00 ± 0.19 , 6.32 ± 0.14 and 5.47 ± 0.01 (in unit $\times 10^{-12} \text{ cm}^3 \text{ molecule}^{-1} \text{ s}^{-1}$, result with *n*-hexane is plotted in SI), respectively (rate constant of reference compounds refers to Atkinson [27]). Since Crawford et al. (*n*-octane and *n*-nonane) and Wilson et al. (di- and tri-methylpentanes and *n*-octane) used higher hydrocarbon molecules as reference compounds, their results of rate constants for *n*-heptane were expected to be lower than ours. Based on the discussions of this work, there are

several possible Arrhenius expressions for *n*-hexane, therefore, we choose *n*-pentane as our reference compound, for which a more comprehensive understanding of temperature-dependence is available. This explains why our data are higher than the existing results. However, more experimental research, especially with absolute measurements is needed to clarify the real reaction rate constant of OH radicals with *n*-heptane at low temperature. Our results for *n*-octane and *n*-nonane are consistent with previous results by Li et al. [28]. This study provides more open questions than a comprehensive understanding of gas-phase reactions of OH with *n*-alkanes below 290 K until precise determinations of absolute rate constants for the higher alkanes become available. The result for cyclooctane confirms the data from Sprengnether et al. [31], however, data at higher temperatures are desirable to validate the Arrhenius expression over a wider temperature range.

Our results for *n*-octane and *n*-nonane are consistent with previous results by Li et al. [28]. This study will help to provide a more comprehensive understanding of gas-phase reactions of OH with *n*-alkanes below 290 K. The result for cyclooctane confirms the data from Sprengnether et al. [31], however, data at higher temperatures are desirable to validate the Arrhenius expression over a wider temperature range.

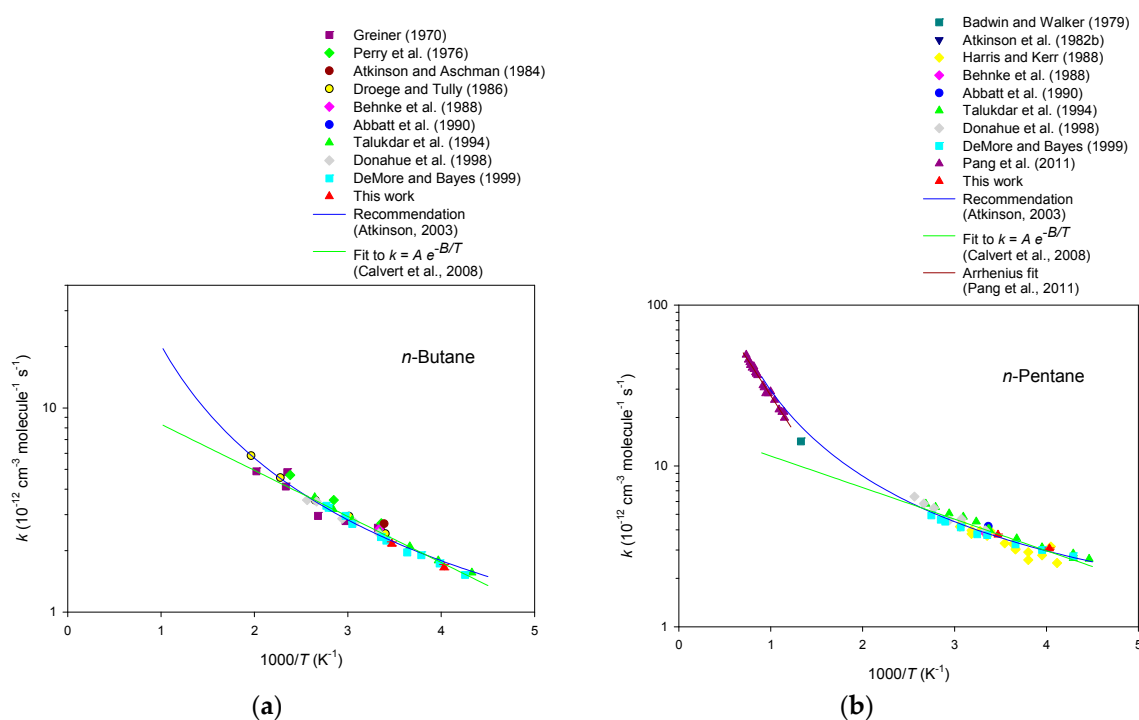


Figure 4. Cont.

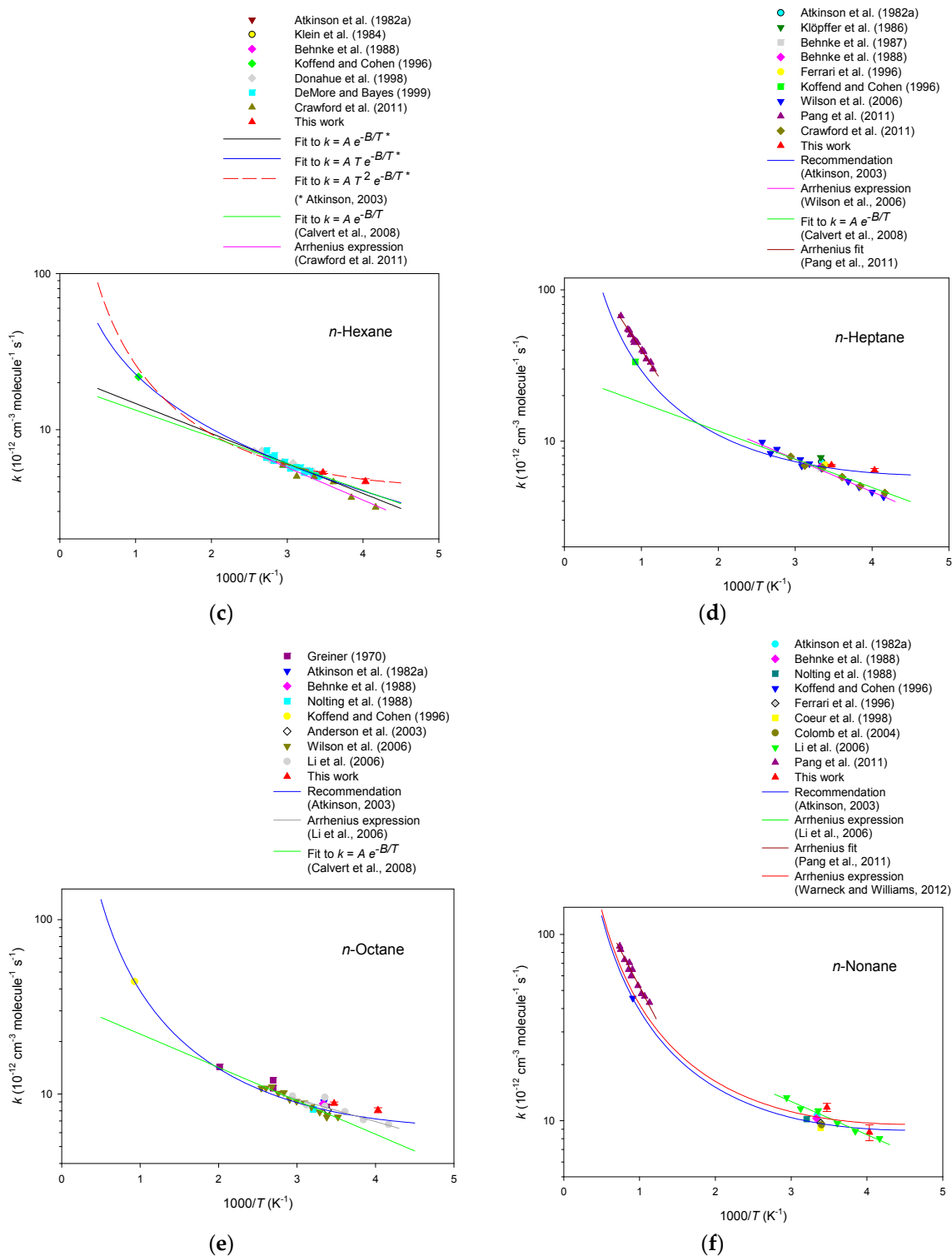


Figure 4. Cont.

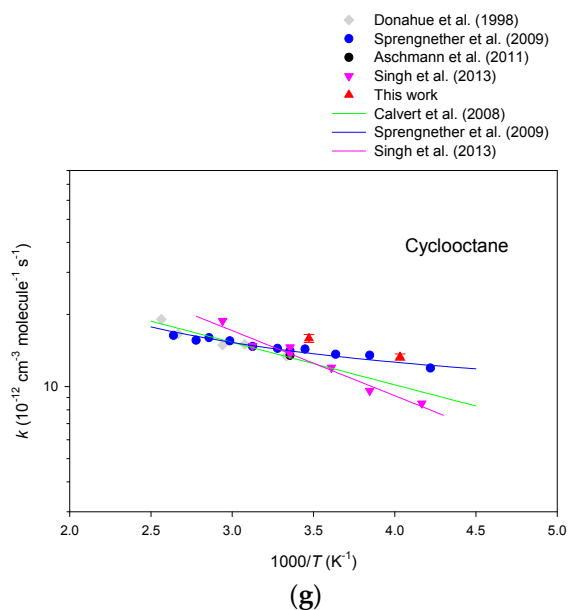


Figure 4. Arrhenius plots of the rate data for the reaction of OH radicals with straight-chain alkanes and cyclooctane in comparison with previous studies [25,39–49].

(2) Figure 5 shows the Arrhenius plot for the reaction of branched-chain alkanes with OH radicals. For the first time, we report the rate constant below 290 K for the reactions of OH radicals with 2,2,4-trimethylpentane, 2,2-dimethylpentane, 2,2,3,3-tetramethylbutane and 2,2-dimethylhexane. The reaction rate constant data for 2,2-dimethylbutane, 2,2,4-trimethylpentane and 2,2,3,3-tetramethylbutane are consistent with previous results and follow the existing Arrhenius expressions (or non-linear fit) as well. For 2,2-dimethylbutane, we give an estimated Arrhenius fit to $k = ATe^{-B/T}$ by applying the value of activation energy ($B = 445$ K) estimated by Kwok and Atkinson [50] and obtain an expression of $k = 3.33 \times 10^{-14} T e^{-445/T} \text{ cm}^3 \text{ molecule}^{-1} \text{ s}^{-1}$. For 2,2-dimethylpentane and 2,2-dimethylhexane, calculated values (based on a structure-activity relationship (SAR) [51]) at room temperature are given for these two compounds to evaluate the temperature dependence. The results of 2,2-dimethylpentane fit well to the non-linear fit provided by Badra and Farooq [52]. A SAR estimation is given for 2,2-dimethylhexane, and our data fall very close to the estimation line. Nevertheless, in order to give a more accurate evaluation of the temperature dependence of 2,2-dimethylhexane, more experimental data are needed to establish the temperature dependence and hereafter to develop the Arrhenius expression for this compound.

(3) Regarding the activated aromatic hydrocarbons, our rate data points at 288 K and 248 K coincide well with the existing data points, showing that the rate constant for these reactions had a negative dependence on temperature at $T \leq 298$ K, which indicates a coherent pathway of electrophilic addition of the OH radical to the aromatic ring [23]. Combining our results with the available literature data (Figure 5), we here give Arrhenius expressions for *o*-xylene, *p*-xylene and ethylbenzene: $6.24 \times 10^{-12} e^{(203 \pm 126)/T} \text{ cm}^3 \text{ molecule}^{-1} \text{ s}^{-1}$, $1.03 \times 10^{-11} e^{(62 \pm 116)/T} \text{ cm}^3 \text{ molecule}^{-1} \text{ s}^{-1}$ and $6.90 \times 10^{-12} e^{(8 \pm 135)/T} \text{ cm}^3 \text{ molecule}^{-1} \text{ s}^{-1}$, respectively (SI, Table S3). All previously reported data points for ethylbenzene existed around room temperature, which caused great uncertainties in determining the activation energy. Further investigations at other temperatures lower than 298 K are required to give a more precise evaluation of the Arrhenius expression for ethylbenzene.

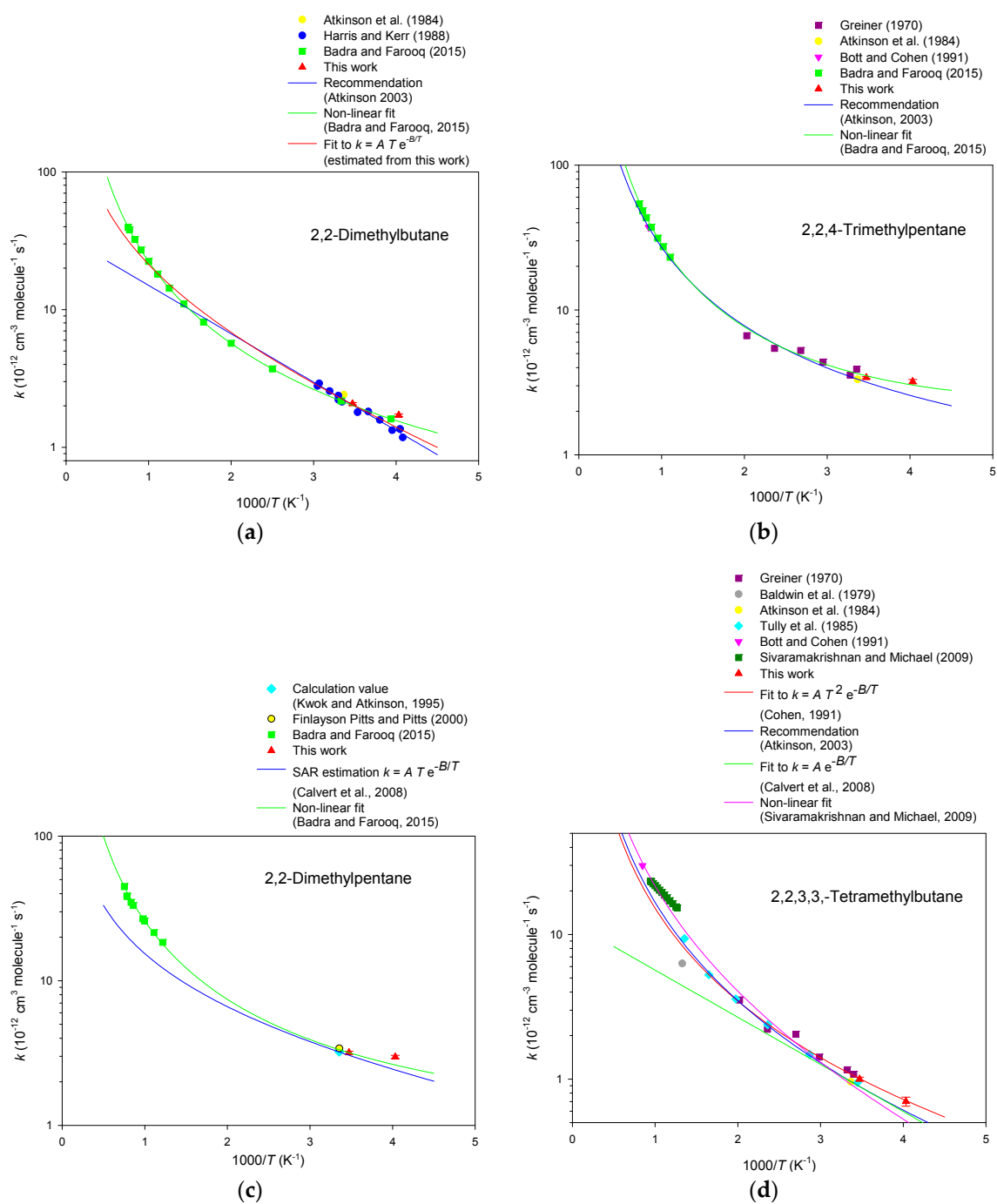


Figure 5. Cont.

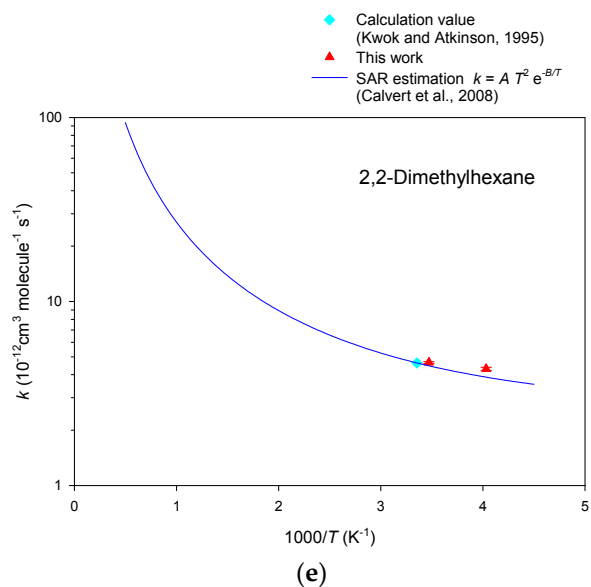


Figure 5. Arrhenius plots of the rate data for the reaction of OH radicals with branched-chain alkanes [47,53–58].

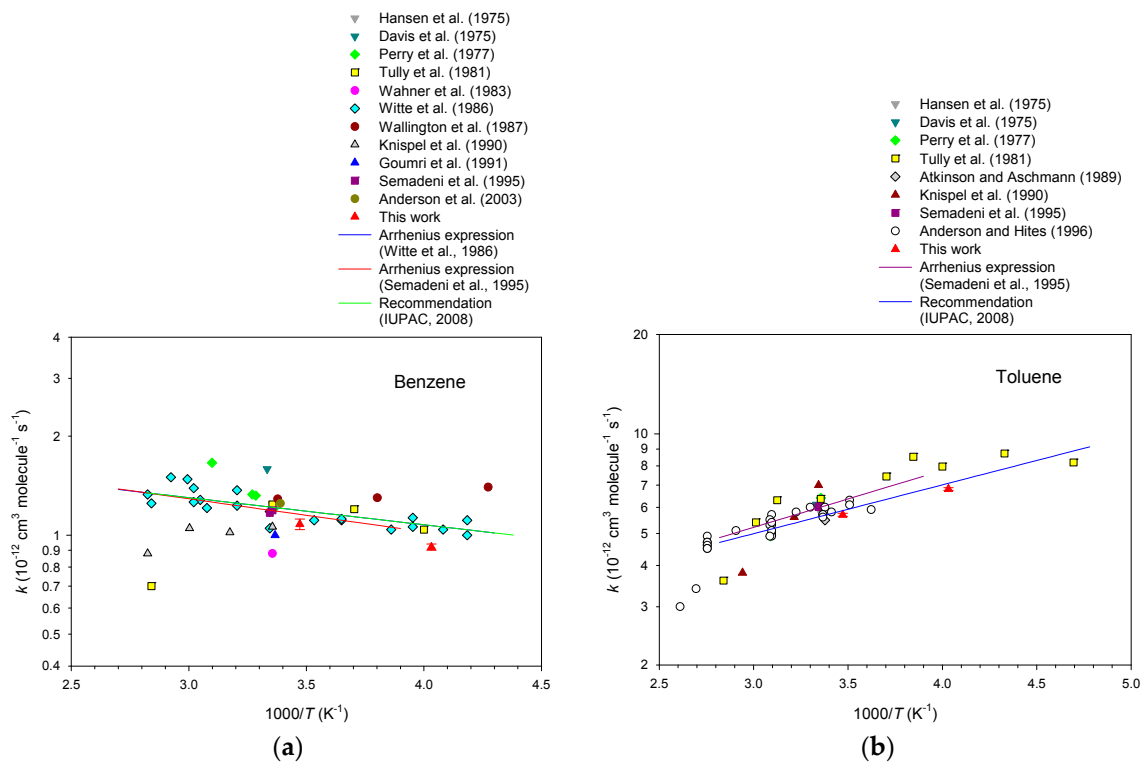


Figure 6. Cont.

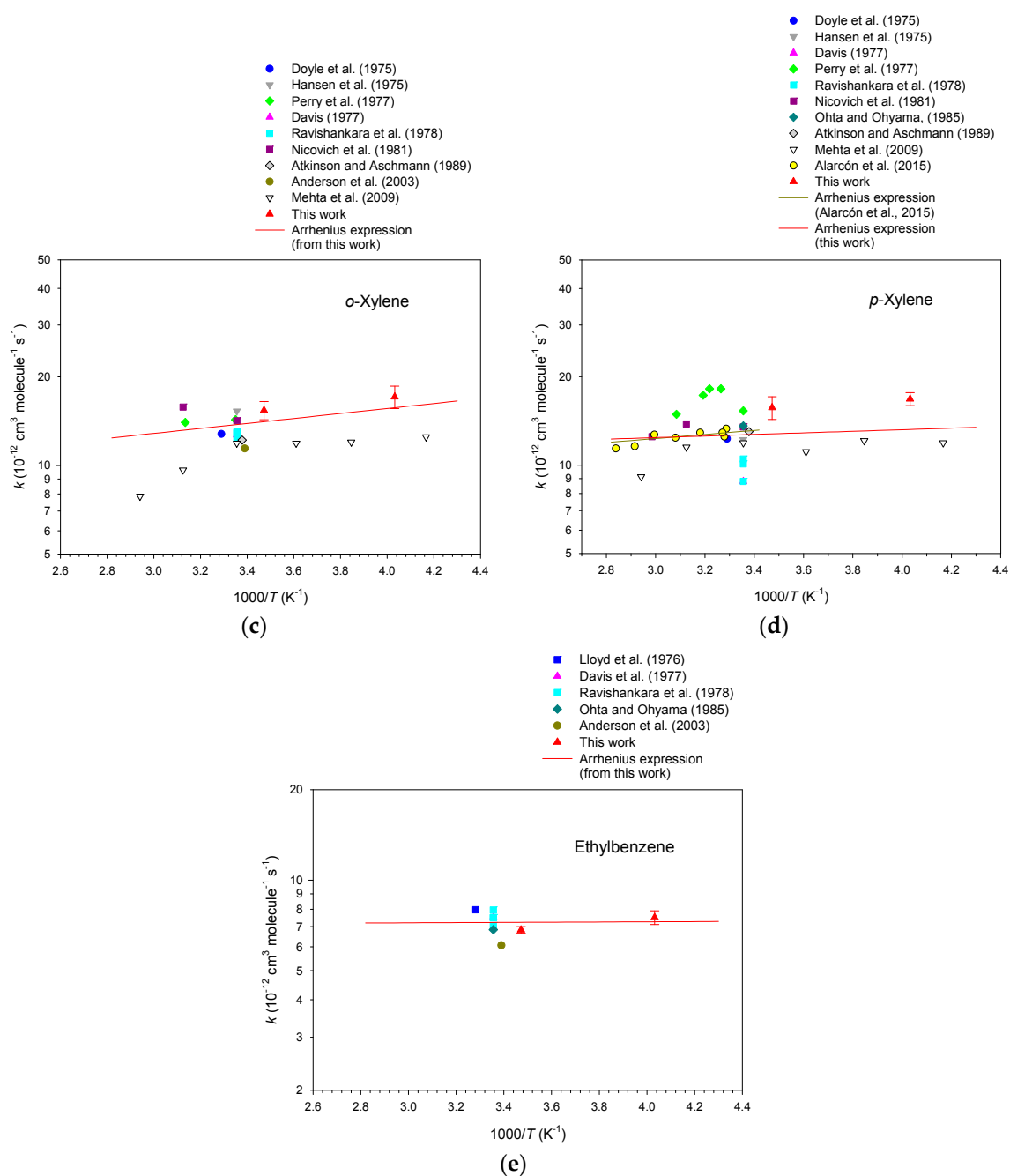


Figure 6. Arrhenius plots of the rate data for the reaction of OH radicals with aromatic hydrocarbons [33,34,59–67].

5. Conclusions

In summary, this study has reported the rate constant of gaseous OH radicals with 17 hydrocarbons at 288 K and 248 K. The results have proven the capability of our simulation chamber for atmospheric chemistry study. Data obtained from this work are consistent with previous studies, supplementing the existing database. Our data on *n*-hexane agree well with the recommended Arrhenius expression ($k = 1.82 \times 10^{-17} T^2 e^{361/T} \text{ cm}^3 \text{ molecule}^{-1} \text{ s}^{-1}$ [4]) over the temperature range from 290 to 970 K. Using the activation energy recommended by Kwok and Atkinson [50] for 2,2-dimethylbutane from an SAR calculation ($B = 445 \text{ K}$), we obtain the Arrhenius expression $k = 3.33 \times 10^{-14} T e^{-445/T} \text{ cm}^3 \text{ molecule}^{-1} \text{ s}^{-1}$. This study reports experimental results for the rate constant of the gas phase reaction of 2,2-dimethylhexane with OH, extending the homologous series of the 2,2-dimethylalkanes.

Data obtained from this study will help to give a more comprehensive understanding to evaluate the atmospheric behavior of this compound.

For aromatic hydrocarbons, we reported the first determination of a rate constant for the reaction of OH radicals with ethylbenzene below the atmospheric sea level temperature ($T \leq 288$ K). Our data points agree with the existing results from previous research. Results from this work will help to evaluate the atmospheric degradations of *n*-alkanes, branched-chain alkanes, and aromatic hydrocarbons with better precision, especially in the lower and middle troposphere.

Supplementary Materials: The following are available online at <http://www.mdpi.com/2073-4433/9/8/320/s1>, Figure S1: Schematic flowchart of the sample enrichment system connected with gas chromatographic analysis of the gas phase in the smog chamber, Figure S2: Dosage of methyl nitrite into the smog chamber, using a twin of gas containers. This method warrants a fairly constant production of OH, Figure S3: Decrease of the hydrocarbon concentrations (normalized by *n*-perfluorohexane) by the reaction with OH during a smog chamber run at 248 K, Figure S4: Plots of $\ln(c_0/c_t)$ of hydrocarbons versus toluene (reference substance) from data points of three experimental runs at 288 K, respectively (∇ , \circ and \square distinguish data points from different experimental runs), Figure S5: Plots of $\ln(c_0/c_t)$ of hydrocarbons versus toluene (reference substance) from data points of two experimental runs at 248 K, respectively (∇ and \circ distinguish data points from different experimental runs), Figure S6: Arrhenius plots of the rate constant for the reaction of OH radicals with *n*-heptane, Table S1: Studies below room temperature for the reaction of OH radicals with hydrocarbons, Table S2: Rate constants for the reaction of OH radicals with hydrocarbons at 248 K, Table S3: Arrhenius parameters *A* and *B* corresponding to the equation $k_{OH} = Ae^{(-B/T)}$.

Author Contributions: Conceptualization, C.Z.; Experiments, L.H. and F.S.; Data Analysis, L.H. and F.S.; Writing-Original Draft Preparation, L.H.; Writing-Review & Editing, L.H., F.S. and C.Z.; Supervision, C.Z.; Funding Acquisition, C.Z.

Funding: This research was funded by the European Community through the EUROCHAMP project. This publication was funded by the German Research Foundation (DFG) and the University of Bayreuth in the funding program "Open Access Publishing".

Acknowledgments: This work is in memoriam to Heinz-Ulrich Krüger (+) for his enormous technical support and discussions for the primary data.

Conflicts of Interest: The authors declare no conflict of interest.

References

1. Koppmann, R. Chemistry of Volatile Organic Compounds in the Atmosphere. In *Handbook of Hydrocarbon and Lipid Microbiology*; Springer: Heidelberg, Germany, 2010; pp. 267–277.
2. Atkinson, R. Atmospheric Chemistry of VOCs and NO_x. *Atmos. Environ.* **2000**, *34*, 2063–2101. [[CrossRef](#)]
3. Carter, W.P.L.; Pierce, J.A.; Luo, D.; Malkina, I.L. Environmental Chamber Study of Maximum Incremental Reactivities of Volatile Organic Compounds. *Atmos. Environ.* **1995**, *29*, 2499–2511. [[CrossRef](#)]
4. DeMore, W.B.; Bayes, K.D. Rate Constants for the Reactions of Hydroxyl Radical with Several Alkanes, Cycloalkanes, and Dimethyl Ether. *J. Phys. Chem. A* **1999**, *103*, 2649–2654. [[CrossRef](#)]
5. Doyle, G.L.; Lloyd, A.C.; Darnall, K.R.; Winer, A.M.; Pitts, J.N., Jr. Gas Phase Kinetic Study of Relative Rates of Reaction of Selected Aromatic Compounds with Hydroxyl Radicals in an Environmental Chamber. *Environ. Sci. Technol.* **1975**, *9*, 237–241. [[CrossRef](#)]
6. Greiner, N.R. Hydroxyl Radical Kinetics by Kinetic Spectroscopy. VI. Reactions with Alkanes in the Range 300–500 K. *J. Chem. Phys.* **1970**, *53*, 1070–1076. [[CrossRef](#)]
7. Hansen, D.A.; Atkinson, R.; Pitts, J.N. Rate Constants for the Reaction of Hydroxyl Radicals with a Series of Aromatic Hydrocarbons. *J. Phys. Chem.* **1975**, *79*, 1763–1766. [[CrossRef](#)]
8. Koffend, J.B.; Cohen, N. Shock Tube Study of OH Reactions with Linear Hydrocarbons near 1100 K. *Int. J. Chem. Kinet.* **1996**, *28*, 79–87. [[CrossRef](#)]
9. Nicovich, J.M.; Thompson, R.L.; Ravishankara, A.R. Kinetics of the Reactions of the Hydroxyl Radical with Xylenes. *J. Phys. Chem.* **1981**, *85*, 2913–2916. [[CrossRef](#)]
10. Nolting, F.; Behnke, W.; Zetzsch, C. A Smog Chamber for Studies of the Reactions of Terpenes and Alkanes with Ozone and OH. *J. Atmos. Chem.* **1988**, *6*, 47–59. [[CrossRef](#)]
11. Perry, R.A.; Atkinson, R.; Pitts, J.N. Kinetics and Mechanism of the Gas Phase Reaction of Hydroxyl Radicals with Aromatic Hydrocarbons over the Temperature Range 296–473 K. *J. Phys. Chem.* **1977**, *81*, 296–304. [[CrossRef](#)]

12. Tully, F.P.; Koszykowski, M.L.; Stephen Binkley, J. Hydrogen-Atom Abstraction from Alkanes by OH. I. Neopentane and Neooctane. *Symp. Int. Combust.* **1985**, *20*, 715–721. [CrossRef]
13. Atkinson, R. Kinetics and Mechanisms of the Gas-Phase Reactions of the Hydroxyl Radical with Organic Compounds. *J. Phys. Chem. Ref. Data* **1989**. Available online: <https://srd.nist.gov/JPCRD/jpcrdM1.pdf> (accessed on 8 January 2018).
14. Finlayson, B.J.; Pitts, J.N. Photochemistry of the Polluted Troposphere. *Science* **1976**, *192*, 111–119. [CrossRef] [PubMed]
15. Hecht, T.A.; Seinfeld, J.H.; Dodge, M.C. Generalized Kinetic Mechanism for Photochemical Smog. *Environ. Sci. Technol.* **1974**, *8*, 327–339. [CrossRef]
16. Pitts, J.N., Jr.; Darnall, K.; Winer, A.; McAfee, J. Mechanisms of Photochemical Reactions in Urban Air. Volume II. Chamber Studies. 1977. Available online: https://cfpub.epa.gov/si/si_public_record_Report.cfm?dirEntryId=40180 (accessed on 8 January 2018).
17. Rohrer, F.; Bohn, B.; Brauers, T.; Brüning, D.; Johnen, F.-J.; Wahner, A.; Kleffmann, J. Characterisation of the Photolytic HONO-Source in the Atmosphere Simulation Chamber SAPHIR. *Atmos. Chem. Phys.* **2005**, *5*, 2189–2201. [CrossRef]
18. Zador, J.; Turányi, T.; Wirtz, K.; Pilling, M.J. Measurement and Investigation of Chamber Radical Sources in the European Photoreactor (EUPHORE). *J. Atmos. Chem.* **2006**, *55*, 147–166. [CrossRef]
19. Karl, M.; Brauers, T.; Dorn, H.-P.; Holland, F.; Komenda, M.; Poppe, D.; Rohrer, F.; Rupp, L.; Schaub, A.; Wahner, A. Kinetic Study of the OH-isoprene and O₃-isoprene Reaction in the Atmosphere Simulation Chamber, SAPHIR. *Geophys. Res. Lett.* **2004**, *31*. [CrossRef]
20. Wang, X.; Liu, T.; Bernard, F.; Ding, X.; Wen, S.; Zhang, Y.; Zhang, Z.; He, Q.; Lü, S.; Chen, J.; et al. Design and Characterization of a Smog Chamber for Studying Gas-Phase Chemical Mechanisms and Aerosol Formation. *Atmos. Meas. Tech.* **2014**, *7*, 301–313. [CrossRef]
21. Harris, S.J.; Kerr, J.A. Relative Rate Measurements of Some Reactions of Hydroxyl Radicals with Alkanes Studied under Atmospheric Conditions. *Int. J. Chem. Kinet.* **1988**, *20*, 939–955. [CrossRef]
22. Talukdar, R.K.; Mellouki, A.; Gierczak, T.; Barone, S.; Chiang, S.-Y.; Ravishankara, A.R. Kinetics of the Reactions of OH with Alkanes. *Int. J. Chem. Kinet.* **1994**, *26*, 973–990. [CrossRef]
23. Tully, F.P.; Ravishankara, A.R.; Thompson, R.L.; Nicovich, J.M.; Shah, R.C.; Kreutter, N.M.; Wine, P.H. Kinetics of the Reactions of Hydroxyl Radical with Benzene and Toluene. *J. Phys. Chem.* **1981**, *85*, 2262–2269. [CrossRef]
24. Mohanakumar, K. *Stratosphere Troposphere Interactions: An Introduction*; Springer: Dordrecht, The Netherlands, 2008; Available online: https://books.google.com.hk/books?hl=zh-TW&lr=&id=pAQDbLQXnksC&oi=fnd&pg=PR7&dq=Stratosphere+Troposphere+Interactions:+An+Introduction&ots=30W_Js-QWU&sig=6KPUEgpfid-54aoOID9vU94VTeIM&redir_esc=y#v=onepage&q=Stratosphere%20Troposphere%20Interactions%3A%20An%20Introduction&f=false (accessed on 8 January 2018).
25. Droege, A.T.; Tully, F.P. Hydrogen Atom Abstraction from Alkanes by Hydroxyl. 5. *n*-Butane. *J. Phys. Chem.* **1986**, *90*, 5937–5941. [CrossRef]
26. Donahue, N.M.; Clarke, J.S. Fitting Multiple Datasets in Kinetics: *N*-Butane + OH → Products. *Int. J. Chem. Kinet.* **2004**, *36*, 259–272. [CrossRef]
27. Atkinson, R. Kinetics of the Gas-Phase Reactions of OH Radicals with Alkanes and Cycloalkanes. *Atmos. Chem. Phys.* **2003**, *3*, 2233–2307. [CrossRef]
28. Li, Z.; Singh, S.; Woodward, W.; Dang, L. Kinetics Study of OH Radical Reactions with *N*-Octane, *n*-Nonane, and *n*-Decane at 240–340 K Using the Relative Rate/Discharge Flow/Mass Spectrometry Technique. *J. Phys. Chem. A* **2006**, *110*, 12150–12157. [CrossRef] [PubMed]
29. Crawford, M.A.; Dang, B.; Hoang, J.; Li, Z. Kinetic Study of OH Radical Reaction with *N*-Heptane and *n*-Hexane at 240–340K Using the Relative Rate/Discharge Flow/Mass Spectrometry (RR/DF/MS) Technique. *Int. J. Chem. Kinet.* **2011**, *43*, 489–497. [CrossRef]
30. Wilson, E.W.; Hamilton, W.A.; Kennington, H.R.; Evans, B.; Scott, N.W.; DeMore, W.B. Measurement and Estimation of Rate Constants for the Reactions of Hydroxyl Radical with Several Alkanes and Cycloalkanes. *J. Phys. Chem. A* **2006**, *110*, 3593–3604. [CrossRef] [PubMed]
31. Sprengnether, M.M.; Demerjian, K.L.; Dransfield, T.J.; Clarke, J.S.; Anderson, J.G.; Donahue, N.M. Rate Constants of Nine C₆–C₉ Alkanes with OH from 230 to 379 K: Chemical Tracers for [OH]. *J. Phys. Chem. A* **2009**, *113*, 5030–5038. [CrossRef] [PubMed]

32. Singh, S.; de Leon, M.F.; Li, Z. Kinetics Study of the Reaction of OH Radicals with C5–C8 Cycloalkanes at 240–340 K Using the Relative Rate/Discharge Flow/Mass Spectrometry Technique. *J. Phys. Chem. A* **2013**, *117*, 10863–10872. [[CrossRef](#)] [[PubMed](#)]
33. Witte, F.; Urbanik, E.; Zetzsch, C. Temperature Dependence of the Rate Constants for the Addition of Hydroxyl to Benzene and to Some Monosubstituted Aromatics (Aniline, Bromobenzene, and Nitrobenzene) and the Unimolecular Decay of the Adducts. Part 2. Kinetics into a Quasi-Equilibrium. *J. Phys. Chem.* **1986**, *90*, 3251–3259. [[CrossRef](#)]
34. Mehta, D.; Nguyen, A.; Montenegro, A.; Li, Z. A Kinetic Study of the Reaction of OH with Xylenes Using the Relative Rate/Discharge Flow/Mass Spectrometry Technique. *J. Phys. Chem. A* **2009**, *113*, 12942–12951. [[CrossRef](#)] [[PubMed](#)]
35. Alarcón, P.; Bohn, B.; Zetzsch, C. Kinetic and Mechanistic Study of the Reaction of OH Radicals with Methylated Benzenes: 1,4-Dimethyl-, 1,3,5-Trimethyl-, 1,2,4,5-, 1,2,3,5- and 1,2,3,4-Tetramethyl-, Pentamethyl-, and Hexamethylbenzene. *Phys. Chem. Chem. Phys.* **2015**, *17*, 13053–13065. [[CrossRef](#)] [[PubMed](#)]
36. Warneck, P. *Chemistry of the Natural Atmosphere*, 2nd ed.; Academic Press: San Diego, CA, USA, 1999.
37. IUPAC. Preferred Value for Toluene of the IUPAC Task Group on Atmospheric Chemical Kinetic Data Evaluation. Available online: <http://Iupac.Pole-Ether.Fr/> (accessed on 8 January 2018).
38. Doumaux, A.R.; Downey, J.J.M.; Henry, J.P.; Hurt, J.M. Preparation of Methyl or Ethyl Nitrite from the Corresponding Alcohols in a Vapor Phase Process. European Patent No. EP0057143B1, 23 January 1981.
39. Donahue, N.M.; Anderson, J.G.; Demerjian, K.L. New Rate Constants for Ten OH Alkane Reactions from 300 to 400 K: An Assessment of Accuracy. *J. Phys. Chem. A* **1998**, *102*, 3121–3126. [[CrossRef](#)]
40. Abbatt, J.P.D.; Demerjian, K.L.; Anderson, J.G. A New Approach to Free-Radical Kinetics: Radially and Axially Resolved High-Pressure Discharge Flow with Results for Hydroxyl + (Ethane, Propane, *n*-Butane, *n*-Pentane). *J. Phys. Chem.* **1990**, *94*, 4566–4575. [[CrossRef](#)]
41. Behnke, W.; Holländer, W.; Koch, W.; Nolting, F.; Zetzsch, C. A Smog Chamber for Studies of the Photochemical Degradation of Chemicals in the Presence of Aerosols. *Atmos. Environ. (1967)* **1988**, *22*, 1113–1120. [[CrossRef](#)]
42. Atkinson, R.; Aschmann, S.M. Rate Constants for the Reaction of OH Radicals with a Series of Alkenes and Dialkenes at 295 ± 1 K. *Int. J. Chem. Kinet.* **1984**, *16*, 1175–1186. [[CrossRef](#)]
43. Atkinson, R.; Aschmann, S.M.; Carter, W.P.L.; Winer, A.M.; Pitts, J.N. Kinetics of the Reactions of OH Radicals with *N*-Alkanes at 299 ± 2 K. *Int. J. Chem. Kinet.* **1982**, *14*, 781–788. [[CrossRef](#)]
44. Ferrari, C.; Roche, A.; Jacob, V.; Foster, P.; Baussand, P. Kinetics of the Reaction of OH Radicals with a Series of Esters under Simulated Conditions at 295 K. *Int. J. Chem. Kinet.* **1996**, *28*, 609–614. [[CrossRef](#)]
45. Behnke, W.; Nolting, F.; Zetzsch, C. A Smog Chamber Study on the Impact of Aerosols on the Photodegradation of Chemicals in the Troposphere. *J. Aerosol Sci.* **1987**, *18*, 65–71. [[CrossRef](#)]
46. Coeur, C.; Jacob, V.; Foster, P.; Baussand, P. Rate Constant for the Gas-Phase Reaction of Hydroxyl Radical with the Natural Hydrocarbon Bornyl Acetate. *Int. J. Chem. Kinet.* **1998**, *30*, 497–502. [[CrossRef](#)]
47. Calvert, J.G.; Derwent, R.G.; Orlando, J.J.; Tyndall, G.S.; Wallington, T.J. *Mechanisms of Atmospheric Oxidation of the Alkanes*; Oxford University Press: New York, NY, USA, 2008.
48. Atkinson, R.; Aschmann, S.M.; Winer, A.M.; Pitts, J.N. Rate Constants for the Reaction of OH Radicals with a Series of Alkanes and Alkenes at 299 ± 2 K. *Int. J. Chem. Kinet.* **1982**, *14*, 507–516. [[CrossRef](#)]
49. Pang, G.A.; Hanson, R.K.; Golden, D.M.; Bowman, C.T. High-Temperature Measurements of the Rate Constants for Reactions of OH with a Series of Large Normal Alkanes: *N*-Pentane, *n*-Heptane, and *n*-Nonane. *Zeitschrift für Physikalische Chemie* **2011**, *225*, 1157–1178. [[CrossRef](#)]
50. Kwok, E.S.C.; Atkinson, R. Estimation of Hydroxyl Radical Reaction Rate Constants for Gas-Phase Organic Compounds Using a Structure-Reactivity Relationship: An Update. *Atmos. Environ.* **1995**, *29*, 1685–1695. [[CrossRef](#)]
51. Jenkin, M.E.; Valorso, R.; Aumont, B.; Rickard, A.R.; Wallington, T.J. Estimation of Rate Coefficients and Branching Ratios for Gas-Phase Reactions of OH with Aliphatic Organic Compounds for Use in Automated Mechanism Construction. *Atmos. Chem. Phys.* **2018**, *18*, 9297–9328. [[CrossRef](#)]
52. Badra, J.; Farooq, A. Site-Specific Reaction Rate Constant Measurements for Various Secondary and Tertiary H-Abstraction by OH Radicals. *Combust. Flame* **2015**, *162*, 2034–2044. [[CrossRef](#)]
53. Atkinson, R.; Carter, W.P.L.; Aschmann, S.M.; Winer, A.M.; Pitts, J.N. Kinetics of the Reaction of OH Radicals with a Series of Branched Alkanes at 297 ± 2 K. *Int. J. Chem. Kinet.* **1984**, *16*, 469–481. [[CrossRef](#)]

54. Bott, J.F.; Cohen, N. A Shock Tube Study of the Reactions of the Hydroxyl Radical with Several Combustion Species. *Int. J. Chem. Kinet.* **1991**, *23*, 1075–1094. [[CrossRef](#)]
55. Baldwin, R.R.; Walker, R.W.; Walker, R.W. Addition of 2,2,3-Trimethylbutane to Slowly Reacting Mixtures of Hydrogen and Oxygen at 480 °C. *J. Chem. Soc. Faraday Trans. 1 Phys. Chem. Condens. Phases* **1981**, *77*, 2157–2173. [[CrossRef](#)]
56. Finlayson-Pitts, B.J.; Pitts, J.N., Jr. *Chemistry of the Upper and Lower Atmosphere: Theory, Experiments, and Applications*, 1st ed.; Academic Press: San Diego, CA, USA, 1999.
57. Sivaramakrishnan, R.; Michael, J.V. Rate Constants for OH with Selected Large Alkanes: Shock-Tube Measurements and an Improved Group Scheme. *J. Phys. Chem. A* **2009**, *113*, 5047–5060. [[CrossRef](#)] [[PubMed](#)]
58. Cohen, N. Are Reaction Rate Coefficients Additive? Revised Transition State Theory Calculations for OH + Alkane Reactions. *Int. J. Chem. Kinet.* **1991**, *23*, 397–417. [[CrossRef](#)]
59. Ravishankara, A.R.; Wagner, S.; Fischer, S.; Smith, G.; Schiff, R.; Watson, R.T.; Tesi, G.; Davis, D.D. A Kinetics Study of the Reactions of OH with Several Aromatic and Olefinic Compounds. *Int. J. Chem. Kinet.* **1978**, *10*, 783–804. [[CrossRef](#)]
60. Anderson, R.S.; Czuba, E.; Ernst, D.; Huang, L.; Thompson, A.E.; Rudolph, J. Method for Measuring Carbon Kinetic Isotope Effects of Gas-Phase Reactions of Light Hydrocarbons with the Hydroxyl Radical. *J. Phys. Chem. A* **2003**, *107*, 6191–6199. [[CrossRef](#)]
61. Semadeni, M.; Stocker, D.W.; Kerr, J.A. The Temperature Dependence of the OH Radical Reactions with Some Aromatic Compounds under Simulated Tropospheric Conditions. *Int. J. Chem. Kinet.* **1995**, *27*, 287–304. [[CrossRef](#)]
62. Wallington, T.J.; Neuman, D.M.; Kurylo, M.J. Kinetics of the Gas Phase Reaction of Hydroxyl Radicals with Ethane, Benzene, and a Series of Halogenated Benzenes over the Temperature Range 234–438 K. *Int. J. Chem. Kinet.* **1987**, *19*, 725–739. [[CrossRef](#)]
63. Knispel, R.; Koch, R.; Siese, M.; Zetzsch, C. Adduct Formation of OH Radicals with Benzene, Toluene, and Phenol and Consecutive Reactions of the Adducts with NO_x and O₂. *Berichte der Bunsengesellschaft für Physikalische Chemie* **1990**, *94*, 1375–1379. [[CrossRef](#)]
64. Goumri, A.; Pauwels, J.F.; Devolder, P. Rate of the OH + C₆H₆ + He Reaction in the Fall-off Range by Discharge Flow and OH Resonance Fluorescence. *Can. J. Chem.* **1991**, *69*, 1057–1064. [[CrossRef](#)]
65. Anderson, P.N.; Hites, R.A. OH Radical Reactions: The Major Removal Pathway for Polychlorinated Biphenyls from the Atmosphere. *Environ. Sci. Technol.* **1996**, *30*, 1756–1763. [[CrossRef](#)]
66. Ohta, T.; Ohyama, T. A Set of Rate Constants for the Reactions of OH Radicals with Aromatic Hydrocarbons. *Bull. Chem. Soc. Jpn.* **1985**, *58*, 3029–3030. [[CrossRef](#)]
67. Atkinson, R.; Aschmann, S.M. Rate Constants for the Gas-Phase Reactions of the OH Radical with a Series of Aromatic Hydrocarbons at 296 ± 2 K. *Int. J. Chem. Kinet.* **1989**, *21*, 355–365. [[CrossRef](#)]



© 2018 by the authors. Licensee MDPI, Basel, Switzerland. This article is an open access article distributed under the terms and conditions of the Creative Commons Attribution (CC BY) license (<http://creativecommons.org/licenses/by/4.0/>).